Supporting Information

Separation and Molecular-level Segregation of Complex Alkane Mixtures in Metal-Organic Frameworks

David Dubbeldam[1], Casey J. Galvin[1], Krista S. Walton[2], Donald E. Ellis[3],

*and Randall Q. Snurr[1]**

[1]Department of Chemical and Biological Engineering, Northwestern University,

Evanston, Illinois 60208

[2] Department of Chemical Engineering,1005 Durland Hall, Kansas State University,

Manhattan, Kansas 66506

[3]*Department of Physics and Astronomy, Northwestern University, Evanston, Illinois 60208*

Email: snurr@northwestern.edu

1 MOF structure

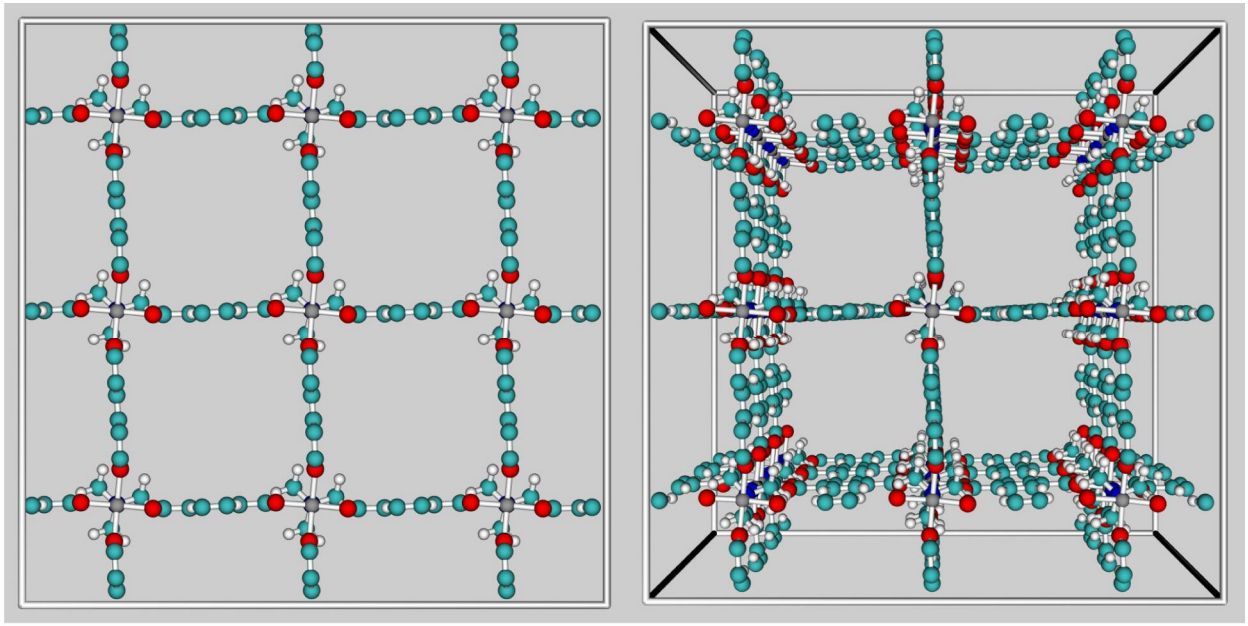

(a) **c** view (orthographic)

(b) **c** view (perspective)

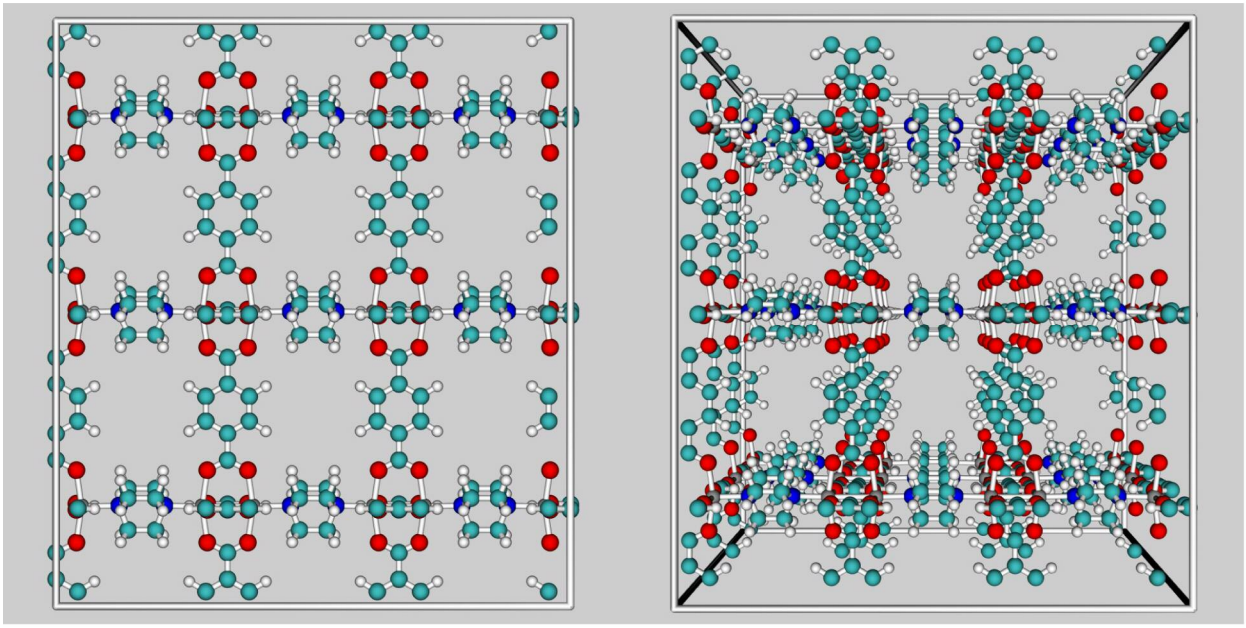

(c) **a** and **b** view (orthographic)

(d) **a** and **b** view (perspective)

Figure S1 The metal-organic framework MOF-**1** as obtained from quantum mechanical structure minimization: (a) and (b) show the view along the rectangular channels of 7.5x7.5 Å, (c) and (d) show the channels running from left to right. Note that the "windows" connecting the rectangular channels in (c) and (d) are about 3.8x4.7 Å, which is too small for longer alkanes to pass easily. Therefore, for the molecules we study, i.e. pentane, hexane, and heptane isomers, the channels are effectively 1-dimensional.

Table S1 The fractional positions of the 54 atoms in the unit cell of MOF-**1** obtained from quantum mechanics (dmol). The experimental unit cell had several positions of the dabco linker super-imposed with fractional occupancies less than 1. Moreover, several versions of the unit cell were provided including benzene and dimethylformamide solvents. The framework is quite flexible and sensitive to the presence of these strongly interacting molecules. Therefore we optimized the unit cell using quantum mechanics to obtain a structure devoid of adsorbates and solvents. The size of the unit cell is **a**=**b**=10.9288, **c**=9.6084 Å, angles $\alpha=\beta=\gamma=90°$.

	type	x	y	z
1	H	0.52564	0.32803	0.37672
2	H	0.62924	0.64450	0.37538
3	H	0.30409	0.57561	0.37573
4	O	0.67246	0.49477	0.88179
5	O	0.30198	0.52543	0.88171
6	H	0.41414	0.69366	0.62442
7	O	0.47326	0.32697	0.88172
8	H	0.36882	0.36388	0.62404
9	O	0.50423	0.69745	0.88156
10	H	0.67643	0.49043	0.62317
11	H	0.62872	0.64505	0.62420
12	H	0.52625	0.32819	0.62297
13	H	0.30389	0.57497	0.62387
14	O	0.30198	0.52551	0.11835
15	H	0.41481	0.69388	0.37593
16	O	0.67247	0.49469	0.11831
17	O	0.50432	0.69742	0.11832
18	H	0.67632	0.48972	0.37723

	type	x	y	z
28	C	0.86065	0.49807	0.00004
29	C	0.47507	0.27484	-0.00003
30	C	0.48161	0.13903	-0.00002
31	C	0.50334	0.74961	-0.00005
32	C	0.49881	0.88552	-0.00003
33	C	0.05077	0.51052	0.87352
34	H	0.10268	0.51361	0.77660
35	C	0.92408	0.50172	0.87355
36	H	0.87216	0.49898	0.77662
37	C	0.48596	0.07564	0.87346
38	H	0.48300	0.12757	0.77655
39	C	0.49487	0.94896	0.87346
40	H	0.49783	0.89702	0.77655
41	C	0.92408	0.50174	0.12653
42	H	0.87216	0.49901	0.22345
43	C	0.05077	0.51054	0.12655
44	H	0.10268	0.51365	0.22347
45	C	0.48591	0.07564	0.12649

19	O	0.47317	0.32699	0.11821
20	H	0.36833	0.36425	0.37630
21	Zn	0.48774	0.51207	0.14773
22	N	0.48635	0.51599	0.36686
23	Zn	0.48774	0.51208	0.85226
24	N	0.48634	0.51601	0.63313
25	C	0.24986	0.52289	0.00003
26	C	0.11415	0.51507	0.00004
27	C	0.72467	0.49490	0.00005

46	H	0.48290	0.12756	0.22341
47	C	0.49483	0.94894	0.12648
48	H	0.49775	0.89699	0.22339
49	C	0.45739	0.39131	0.41987
50	C	0.60872	0.55394	0.41976
51	C	0.39267	0.60351	0.41965
52	C	0.39247	0.60331	0.58033
53	C	0.45764	0.39126	0.58014
54	C	0.60863	0.55424	0.58020

2 Methodology

Configurational Bias Monte Carlo (CBMC)

Conventional Monte Carlo is time-consuming for long chain molecules. The fraction of successful insertions into the sieve is too low. To increase the number of successfully inserted molecules we apply the CBMC technique[1]. In the CBMC scheme a molecule is grown segment by segment. It is convenient to split the total potential energy U of a trial site for the next segment into two parts

$$U = U^{\text{int}} + U^{\text{ext}}$$

The first part is the internal, bonded potential U^{int}, which is used for the generation of trial positions. The second part of the potential, the external potential U^{ext} is used to bias the selection of a site from the set of trial sites. This bias is exactly removed by adjusting the acceptance rules. For each segment we generate a set of *k* trial positions according to the internal energy U^{int} and compute the external energy

$U_i^{\text{ext}}(j)$ of each trial position *j* of segment *i*. In this work the number of trial positions *k* is set to 10. We select one of these trial positions with a probability

$$P_i(j) = \frac{e^{-\beta U_i^{\text{ext}}(j)}}{\sum_{l=1}^{k} e^{-\beta U_i^{\text{ext}}(l)}} = \frac{e^{-\beta U_i^{\text{ext}}(j)}}{w(i)}$$

The selected trial position is added to the chain and the procedure is repeated until the entire molecule has been grown. For this newly grown molecule we compute the so-called Rosenbluth factor

$$W^{\text{new}} = \prod_i w(i)$$

To compute the old Rosenbluth factor W^{old} of an already existing chain, *k*-1 trial positions are generated for each segment. These positions, together with the already existing bond, form the set of *k* trial positions.

Energy computation

We describe in some detail the computation of the energies using CBMC for our molecular united atom model. The total energy U is split into two contributions $U = U^{\text{int}} + U^{\text{ext}}$. The internal energy U^{int} is given by

$$U^{\text{int}} = U^{\text{bond}} + U^{\text{bend}} + U^{\text{torsion}}$$

with

$$U^{\text{bond}} = \sum_{\text{bonds}} \frac{1}{2} k_b (r - r_0)^2$$

$$U^{\text{bend}} = \sum_{\text{bends}} \frac{1}{2} k_b (\theta - \theta_0)^2$$

$$U^{\text{torsion}} = \sum_{\text{torsions}} c_0 + c_1\left[1 + \cos(\phi)\right] + c_2\left[1 - \cos(2\phi)\right] + c_3\left[1 + \cos(3\phi)\right]$$

where k_b is the bond energy constant, r_0 the reference bond length, k_θ the bend energy constant, θ_0 the reference bend angle, ϕ the dihedral angle, and c_n denote the four torsion parameters. The external

energy U^{ext} consists of a guest-guest intermolecular energy U^{gg}, a host-guest interaction U^{hg}, and an intra-molecular Lennard-Jones interaction U^{intra} for beads in a chain separated by more than three bonds

$$U^{\text{ext}} = U^{\text{gg}} + U^{\text{gh}} + U^{\text{intra}}$$

with

$$U^{\text{gg,hg,intra}} = \sum_{\text{LJ-pairs i,j}} 4\varepsilon_{\text{ij}}\left[\left(\frac{\sigma_{ij}}{r_{ij}}\right)^{12} - \left(\frac{\sigma_{ij}}{r_{ij}}\right)^{6}\right]$$

where r_{ij} is the distance between site i and site j, r_{cut}=12.8 Å is the cutoff radius, and $U^{\text{gg,gh,intra}} = 0$ when $r_{ij} > r_{\text{cut}}$. The Lennard-Jones potential consists of two parameters, σ is the size-parameter, and ε is the strength-parameter. The force field is described by the parameters listed in Table 2. Tail corrections and standard Lorentz-Berthelot mixing rules are used.

Table S2 The Lennard-Jones parameters for the framework MOF-**1** (DREIDING[2]) and the adsorbate alkanes (TraPPE[3]). The strength parameter ε/k_B is in units of Kelvin; to convert to kJ/mol multiply by R/1000 with R≈8.314464919 the gas constant. Tail corrections and Lorentz-Berthelot mixing rules are used.

type	ε/k_B [K]	σ [Å]
Zn	27.7	4.04
N	38.977	3.263
O	48.19	3.03
C	47.86	3.47
H	7.65	2.85

	ε/k_B [K]	σ [Å]
CH_4	158.5	3.72
CH_3	108.0	3.76
CH_2	56.0	3.96
CH	17.0	4.67
C	0.8	6.38

Table S3 Stretch, bend, and torsion parameters for alkanes. The parameters are from the TRAPPE force field[3] . The (CH)-(C) torsion is not defined in the TraPPE model and the listed value is taken from Ref. 4.

stretch	r_0 [Å]	k_b/k_B[K/ Å^2]
CHx-CHx	1.54	96500

bend	θ_0	k_θ/k_B[K/rad^2]
CH_X-(CH_2)-CH_Y	114	62500
CH_X-(CH)-CH_Y	112	62500
CH_X-(C)-CH_Y	109.47	62500

torsion	c_0/k_B[K]	c_1/k_B[K]	c_2/k_B[K]	c_3/k_B[K]
CH_X-(CH_2)-(CH_2)-CH_Y	0	335.03	-68.19	791.32
CH_X-(CH_2)-(CH)-CH_Y	-251.06	428.73	-111.85	441.27
CH_X-(CH_2)-(C)-CH_Y	0	0	0	461.29
CH_X-(CH)-(CH)-CH_Y	-251.06	428.73	-111.85	441.27
CH_X-(CH)-(C)-CH_Y	0	0	0	1635.7

Monte Carlo moves

Several Monte Carlo moves are employed during the simulations.

- Displacement move

  A chain is selected at random and given a random displacement. The maximum displacement is adjusted such that 50% of the moves are accepted. The acceptance rule is

$$\mathrm{acc}(\mathrm{old}\rightarrow\mathrm{new})=\min\left(1,e^{-\beta\left(U^{\mathrm{new}}-U^{\mathrm{old}}\right)}\right)$$

  Note that the energy of the new configuration U^{new} and the energy of the old configuration U^{old} only differ in the external energy.

- Rotation move

  A chain is selected at random and given a random rotation. The acceptance rule is

$$\mathrm{acc}(\mathrm{old}\rightarrow\mathrm{new})=\min\left(1,e^{-\beta\left(U^{\mathrm{new}}-U^{\mathrm{old}}\right)}\right)$$

Again, the energy of the new configuration U^{new} and the energy of the old configuration U^{old} only differ in the external energy.

- Insertion move

A chain is grown at a random position. The acceptance rule for insertion of the molecule is given by

$$\text{acc}(\text{N} \rightarrow \text{N}+1) = \min\left(1, \frac{W^{\text{New}} \beta V}{N+1} \frac{f}{\langle W^{\text{IG}} \rangle}\right)$$

where f is the fugacity which is related to the difference in chemical potential of the interacting alkane and an alkane in the ideal gas state. The Rosenbluth weight $\langle W^{\text{IG}} \rangle$ of the reference state of the ideal gas has to be computed in a separate simulation. It can be obtained by a simulation of a single molecule using only the full regrow move at the desired temperature.

- Deletion move

A chain is chosen at random and the old Rosenbluth weight is computed. The acceptance rule for deletion of the molecule is given by

$$\text{acc}(\text{N} \rightarrow \text{N}-1) = \min\left(1, \frac{N}{W^{\text{Old}} \beta V} \frac{\langle W^{\text{IG}} \rangle}{f}\right)$$

- Full regrow move

A chain is selected at random and is completely regrown at a random position. The acceptance rule for full regrow is given by

$$\text{acc}(\text{old} \rightarrow \text{new}) = \min\left(1, \frac{W^{\text{New}}}{W^{\text{Old}}}\right)$$

- Partial regrow move

A chain is selected at random and part of the molecule is regrown. It is decided at random which part of the molecule is regrown. The acceptance rule for partial regrow is

$$\text{acc}(\text{old} \rightarrow \text{new}) = \min\left(1, \frac{W^{\text{New}}}{W^{\text{Old}}}\right)$$

- Identity move

The identity-change trial move[5] is called semi-grand ensemble, but it can also be seen as a special case of the Gibbs ensemble. One of the components is selected at random and an attempt is made to change the identity of a randomly selected molecule of this type (the new type is chosen randomly from all components). The acceptance rule is given by[6]

$$\mathrm{acc}(\mathrm{A}\rightarrow\mathrm{B}) = \min\left(1, \frac{W^{\mathrm{New}}}{W^{\mathrm{Old}}} \frac{f_B}{\left\langle W_B^{\mathrm{IG}} \right\rangle} \frac{\left\langle W_A^{\mathrm{IG}} \right\rangle}{f_A} \frac{N_A}{(N_B+1)}\right)$$

where f_A and f_B are the fugacities of components *A* and *B*, and N_A and N_B are the numbers of molecules of *A* and *B*, respectively.

3 Results: snapshots of the simulations

The snapshot pictures are made with VTK (the Visualization ToolKit)[7]. During a grand-canonical Monte Carlo simulation a 3-dimensional histogram of the positions of all united atom alkane beads is collected (per component). The unit cell is divided into 150x150x150 "voxels". During the simulation the molecules move around in the box, and every cycle (a cycle consists of N Monte Carlo steps; note that the number of molecules N fluctuates during a GCMC simulation) data is collected for the histogram. First a position is mapped back from the full simulation box (3x3x3 unit cells) to the main unit cell, and for every atom the voxel corresponding to the mapped position is incremented. At certain intervals the histogram is written to file so that it can be visualized using VTK. The data is always normalized using the highest occurring voxel value. However, the overall brightness is still influenced by the loading of the specific adsorbate in the mixture. The pictures show 2x2x2 unit cells.

In VTK the data is "volume rendered", more dense regions are less transparent, less dense regions are more transparant. In addition the color changes, less dense regions are grey, more dense are orange, then yellow, and the highest is rendered light blue. The original framework is placed in the picture as a ball-and-stick model, and every position can be related to the framework. We can therefore decipher a

molecular picture of why selectivity occurs. Because we map all the beads we also obtain information on the orientation and alignment of the alkanes. We have made the snapshots at low loading, where there are hardly any adsorbate-adsorbate interactions, and at very high loading. This enables us to determine any relocation of certain types of alkanes.

At low loading, linear alkanes are found uniformly along the channel axis, and the triple branched alkanes are found predominantly sandwiched in between two pairs of opposing bdc linkers. The mono and di-branched molecules show the gradual transition in between these two extremes. A second point worth mentioning is that, when viewed along the channel direction, all molecules are found in the center of the channel. Striking differences are obtained at high loading. Linear alkanes are now only found in between two neighboring bdc groups, and they are not found in the center of the channel, but rather they are aligned to the dabco linker (diagonally in the picture). Chains with linear tails adsorb best while more bulky and branched molecule are adsorbing less and/or are driven out.

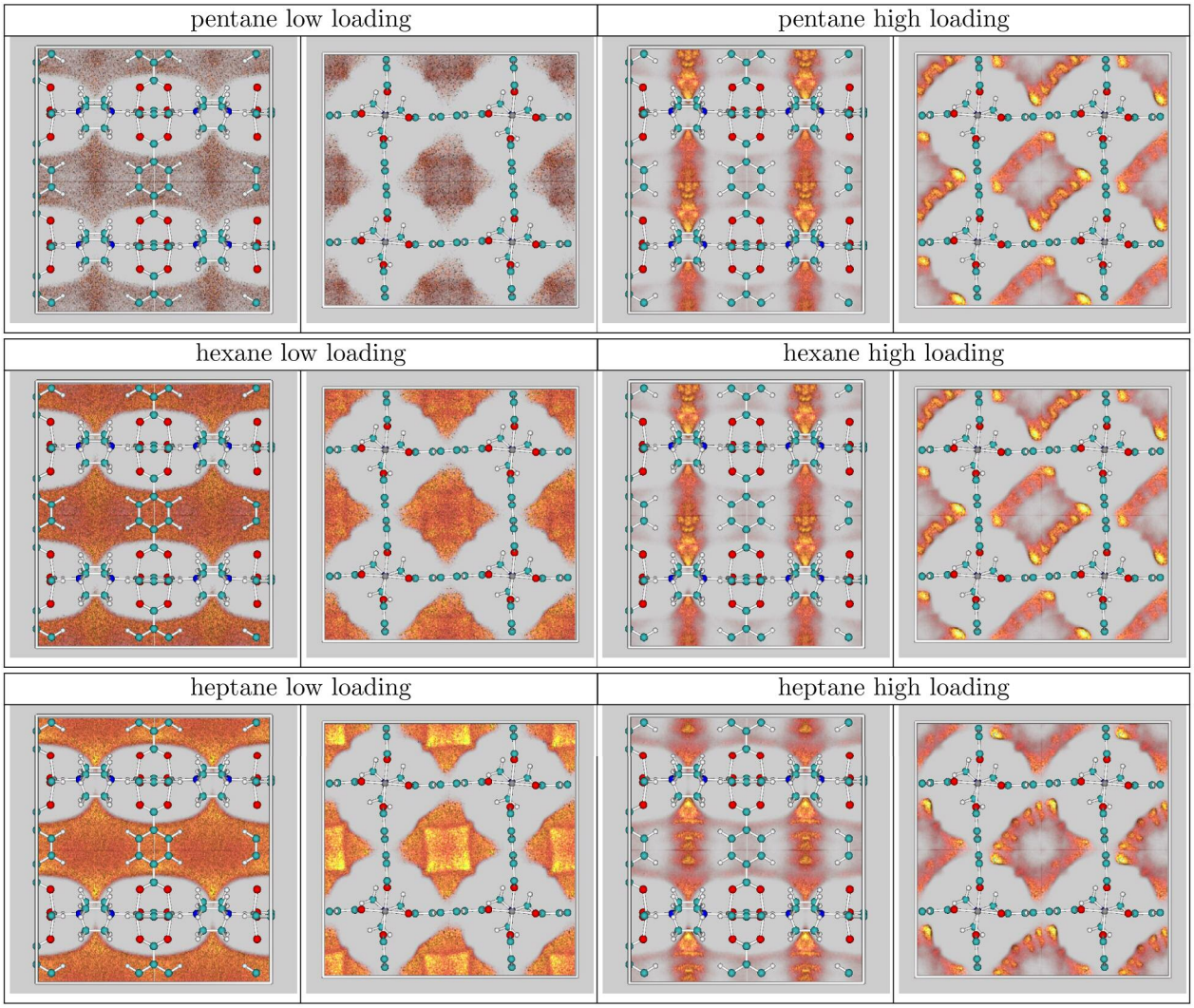

Figure S2 The average positions of all the beads of linear alkanes in a 13-component mixture at low and high loading (298K, 0.5 and 1048576 Pa) in the metal-organic framework MOF-**1**. The left picture is a sideview of the channels, i.e. the channels are running from left to right, the right picture shows the view along the channel.

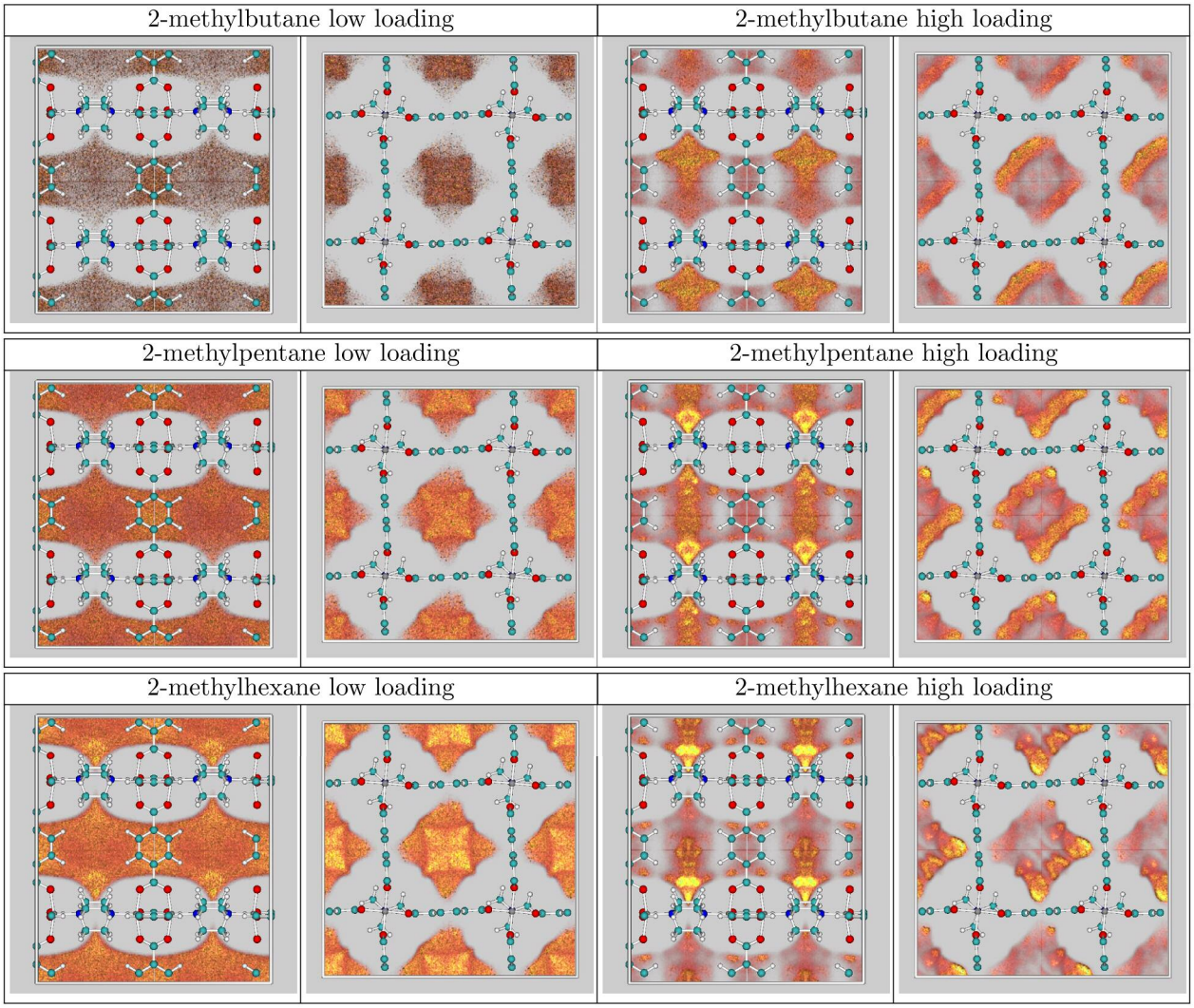

Figure S3 The average positions of all the beads of mono branched (2-methyl-) alkanes in a 13-component mixture at low and high loading (298K, 0.5 and 1048576 Pa) in the metal-organic framework MOF-**1**. The left picture is a sideview of the channels, i.e. the channels are running from left to right, the right picture shows the view along the channel.

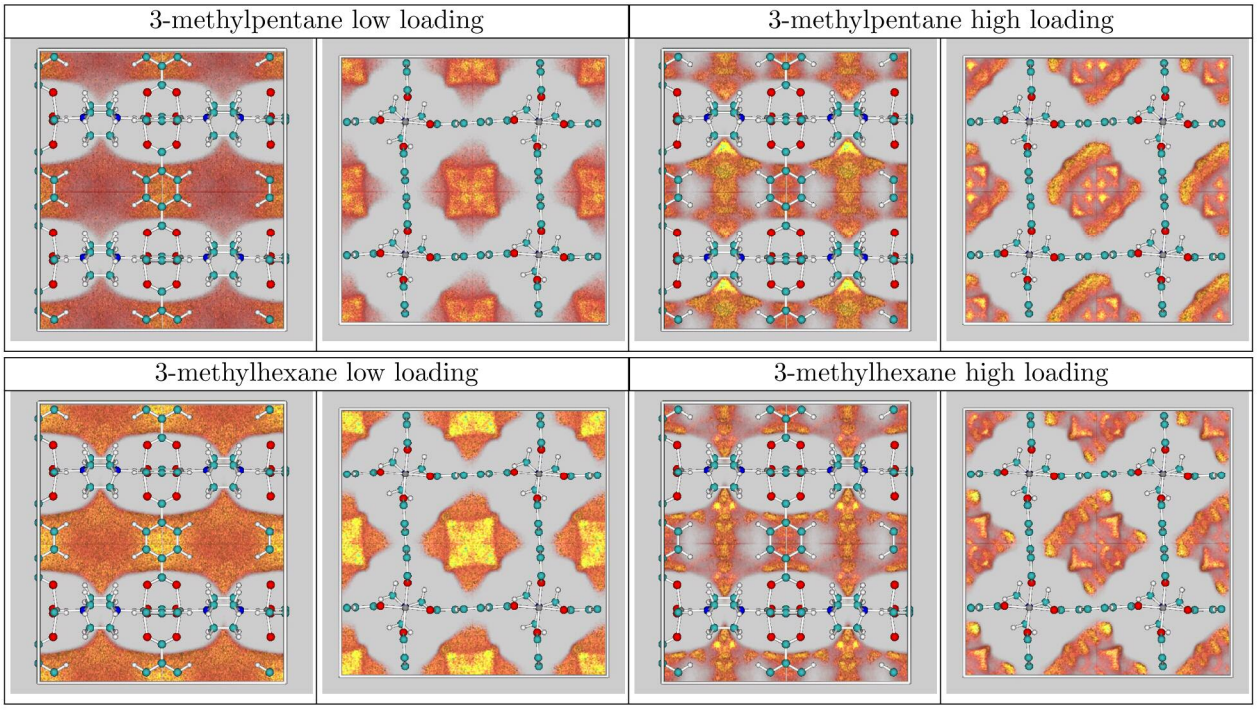

Figure S4 The average positions of all the beads of mono branched (3-methyl-) alkanes in a 13-component mixture at low and high loading (298K, 0.5 and 1048576 Pa) in the metal-organic framework MOF-**1**. The left picture is a sideview of the channels, i.e. the channels are running from left to right, the right picture shows the view along the channel.

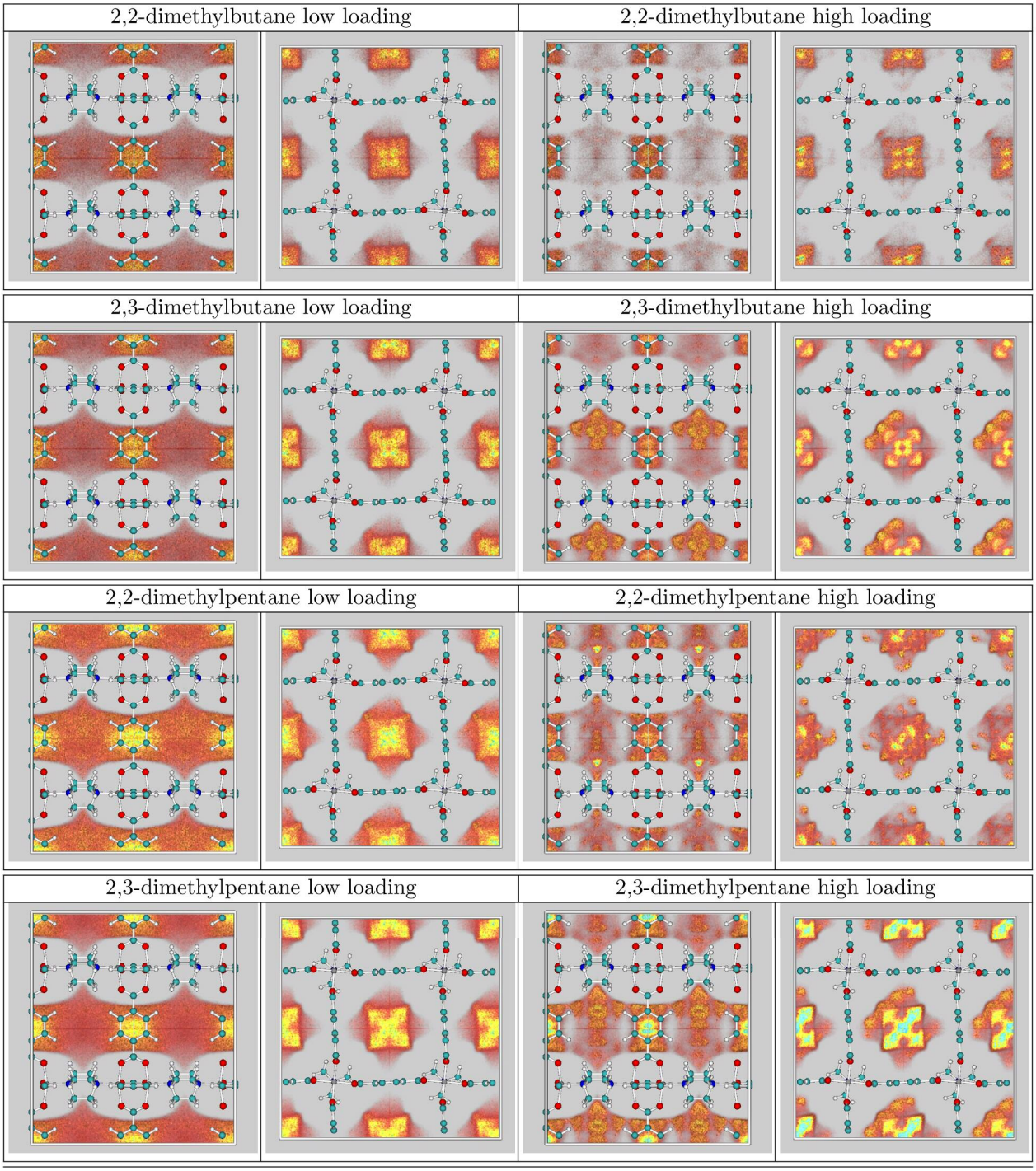

Figure S5 The average positions of all the beads of double branched alkanes in a 13-component mixture at low and high loading (298K, 0.5 and 1048576 Pa) in the metal-organic framework MOF-**1**. The left picture is a sideview of the channels, i.e. the channels are running from left to right, the right picture shows the view along the channel.

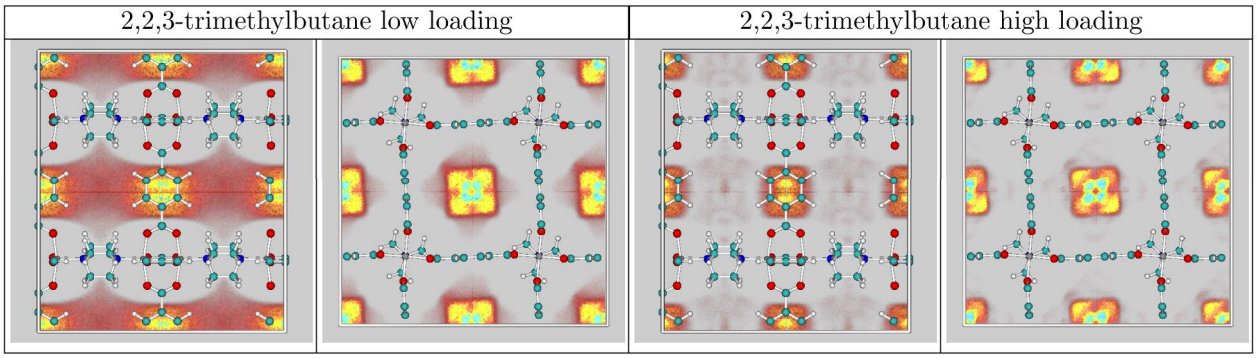

Figure S6 The average positions of all the beads of a triply branched alkane in a 13-component mixture at low and high loading (298K, 0.5 and 1048576 Pa) in the metal-organic framework MOF-1. The left picture is a sideview of the channels, i.e. the channels are running from left to right, the right picture shows the view along the channel.

1 (a) Frenkel, D; Smit, B., *Understanding Molecular Simulation 2nd edition* Academic Press; London, Uk, 2002. (b) Siepmann, J.I. *Mol. Phys.* **1990**, 70, 1145. (c) Siepmann, J.I.; Frenkel, D. *Mol. Phys.* **1992**, 75, 59. (d) Frenkel, D.; Mooij, G.C.A.M.; Smit, B. *J. Phys.: Condens. Matter* **1992**, 4, 3053. (e) Laso, M.; de Pablo, J.J.; Suter, U.W. *J. Chem. Phys.* 1992, 97, 2817. (f) Siepmann, J.I.; McDonald, I.R.; *Mol. Phys.* **1992**, 75, 255. (g) Vlugt, T.J.H.; Krishna, R.; Smit, B.; *J. Phys. Chem. B* **1999**, 103, 1102. (h) Martin, M.G.; Siepmann, J.I.; *J. Phys. Chem. B* **1999**, 103, 4508.

2 Mayo, S.L.; Olafson, B.D.; Goddard, W.A. *J. Phys. Chem.* **1990**, 94, 8897.

3 (a) Martin, M.G.; Siepmann, J.I. *J. Phys. Chem.* 1998, 102, 2569 (b) Martin, M.G.; Siepmann, J.I.; *J. Phys. Chem. B* **1999**, 103, 4508.

4 Natha, S. K.; Khare, R. *J. Chem. Phys.* **2001**, 115, 10837.

5 Martin, M.G.; Siepmann, J.I. *J. Am. Chem. Soc.* **1997**, 119, 8921.

6 Panagiotopoulos, A. Z. *Int. J. Thermophys.* **1989**, 10, 447.

7 (a) Schroeder, W.; Martin. K.; Lorensen, B. *The Visualization Toolkit: an object oriented approach to 3D graphics* Prentice-Hall,Inc; Upper Saddle River, New Jersey 07458, **1996**, (b) http://public.kitware.com/VTK/